Modern Applied Science; Vol. 9, No. 6; 2015
ISSN 1913-1844 E-ISSN 1913-1852
Published by Canadian Center of Science and Education

Investigation of Petrophysical Properties for Yamamma Carbonate Formation

Fadhil Sarhan Kadhim[1,2], Ariffin Samsuri[1], Ahmad Kamal Idris[1], Haider Alwan[3] & Muhammad Hashim[4]

[1] Department of Petroleum Engineering, Faculty of Petroleum and Renewable Energy, Universiti Teknologi Malaysia, 81310, Skudai, Johor, Malaysia

[2] University of Technology, Baghdad, Iraq

[3] Iraqi Drilling Company, Basrah, Iraq

[4] Balochistan University of Information Technology, Engineering and Management Sciences, Quetta, Pakistan

Correspondence: Fadhil Sarhan Kadhim, Universiti Teknologi Malaysia, 81310, Skudai, Johor, Malaysia. Tel: 60-187-902-925. E-mail: skfadhil2@live.utm.my/ fadhilkadhim47@yahoo.com

Received: November 13, 2014 Accepted: December 17, 2014 Online Published: March 25, 2015

doi:10.5539/mas.v9n6p36 URL: http://dx.doi.org/10.5539/mas.v9n6p36

The research is financed by Ministry of Higher Education and Scientific Research-Iraq and Universiti Teknologi Malaysia.

Abstract

Given the knowledge of the rock type, porosity, Archie's parameters and water saturation can be determined by using different logging devices. For example, if a density logging tool is to be used, the rock matrix density must be known in order to determine the porosity. Likewise, using sonic log for porosity determination, the known parameter must be the matrix travel time and for neutron log, the parameter that must correspond to the rock type is the matrix setting for the neutron logging tool. Many equations have been developed over the years based on known physical principles or on empirically derived relationships, which are used to calculate porosity, resistivity, water saturation, and estimate the lithology. NS oilfield is one of giant oilfields in the Middle East, and the formation under study is the Yammama carbonate formation which is one of the deepest hydrocarbons bearing zone in NS oilfield. Neurology software (V 5, 2008) was used to digitize the scanned copies of the available logs. Environmental corrections had been made as per SLB charts 2005. Results show that the Yammama formation consists mainly of limestone, some dolomite as well as the average formation water resistivity (Rw= 0.0179), average mud filtrate resistivity (Rmf= 0.091), and Archie's parameters (m=1.94, n= 2, and a=0.7). While the porosity, true resistivity, and water saturation values with depth of formation were calculated. This study provides the cross-plots, which can be used to determined lithology of this reservoir and investigated petrophysical properties that should use to estimate original oil in place and detected the perforation zones.

Keywords: petrophysical properties, carbonate formation, lithology, porosity, water saturation

1. Introduction

Fluid flow through heterogeneous carbonate reservoirs (limestone and dolomite) is a substantially different process from the flow through the homogeneous sandstone reservoir. This variation is largely cause to the fact that carbonate rocks tend to have a more complex pore system (i.e the interrelationships among depositional lithologies, the geometries of depositional facies, and diagenesis) than sandstone [1]. Middle East carbonate reservoirs contain supergiant oil and gas fields, which cover around fifteen percent of the world's oil reserves [2].

The calculation of water saturation value is one of the most troublesome aspects of log analysis. This value should be calculated, in order to determine the saturations of hydrocarbons in the formations. The saturation exponent (n) and cementation exponent *(m*) are estimated from well logs and core data analysis or from prior experience with local formation characteristics. The resistivity of a formation for its matrix and fluid (water and hydrocarbon) in the pores is true resistivity (R_t), which is usually obtained from deep resistivity log reading such as; Deep Induction Log (DIL) or Deep Lateral Log (DLL). Whereas the mud filtrate resistivity in **the** flushed

zone (R_{mf}.) and the resistivity of the flushing zone (Rxo) are measured by Micro Spherical Focused Logs (MSFL), as well as the resistivity of the flushing zone (Rxo). Practically, the formation water resistivity (R_w) estimates from Spontaneous Potential (SP) log. The porosity (Φ) data can be estimated from several types of porosity logs, for instance; Density, Neutron, or Sonic log [3].

Well logs are considered one of the main sources of data for the geological and petrophysical parameters of reservoir formations. NS oil field is the area of study considered as a giant oil field in the Middle East. Also, it is characterized by carbonate reservoirs. NS oil field has reserves in late Cretaceous Yamamma limestone formation in depth about (3177-3403m) according the results of NS-3, which is the study well.Yamamma formation is widely distributed across the Middle East. The main aim of this study is calculation of petrophysical properties, and as aresult calculate water saturation that should use to estimate original oil in place and detected the perforation zones.

2. Methodology

Neura-Log software (NL-V 5,2008) used to digitize the scanned copies of logs for studied well, so the results are LAS files, which loaded to the Interactive Petrophysics software (IP- V3.5, 2008), then the reading measurements taken as one reading per 0.1524 meters. The log curves are checked to be in depth with each other. All log curves, then depth-matched with the available gamma ray readings that taken as a reference guide for depth matching.

True corresponding between gamma ray readings and other logging tools was clear at formations tops. Environmental corrections were made using the current Schlumberger charts (SLB, 2005), which are supplied to IP as the environmental correction module, actual mud properties, calliper log, hydrostatic pressure and temperature gradient were provided for accurate corrections. Depending on well log data the IP had been used to calculate the petrophysical reservoir rock properties, R_t, R_{xo}, R_w, R_{mf}, Φ, *m*, and n

3. Results

3.1 Porosity Calculations

The density tool responds to the electron density of the material in the formation. Formation bulk density (ρ_b) is a function of matrix density, porosity, and density of fluids in the pores (salt water, fresh water drilling mud, or hydrocarbons). The formula for calculating density-derived porosity is [3]:

$$\Phi_D = \frac{2.71 - \rho_b}{2.71 - \rho_f} \quad \text{.....(1)}$$

Where: $\boldsymbol{\rho}_b$: is the bulk (matrix) density, [2.71 (gm /cc) for limestone, 2.87 (gm /cc) for dolomite and 2.65 (gm /cc) for sandstone], while $\boldsymbol{\rho}_f$: is the fluid density (gm /cc) [for fresh water drilling mud =1 and for salt water mud 1.1].

Neutron logs measure the hydrogen concentration in a formation in clean formations (i.e., shale-free), where the pores are filled with water or oil, therefore hydrogen is concentrated in the fluid-filled pores, energy loss can be related to the formation porosity. Whenever shale is part of the formation matrix the reported neutron porosity (Φ_N) is greater than the actual formation porosity [4]. Sonic tool is a porosity log that measures interval transit time (Δt) of a compressional sound wave traveling through the formation, the interval transit time (Δt) depends upon both lithology and porosity. Wyllie time-average equation may be written as follows [5]:

$$\Phi S = \frac{\Delta t_{\log} - \Delta t_{mat}}{\Delta t_f - \Delta t_{mat}} \quad \text{.....(2)}$$

Where: Φs: is sonic-derived porosity, fraction; Δtma: is the interval transit time in the matrix [Its value is 47.6 μsec/ft for Limestone and 43.5 μsec/ft for dolomite)]; Δtlog: is the interval transit time in the formation, μsec/ft; Δtf: is the interval transit time in the fluid within the formation [For fresh water mud = 189 (μsec/ft); for salt-water mud = 185 (μsec/ft)].

The environmental corrected results for gamma ray, resistivity and porosity logs are shown in Figure (1).Porosity values from neutron, sonic and density logs are illustrated in track 8and 9 in Figure (1). The Computer Processed Interpretation (CPI) results of effective porosity (PHIE) are closed to the core data analysis as shown in Table (1)

and Figures 2, 3, 4, 5, 6, 7 and 8.

3.2 Lithology Determination

A Cross-plot of porosity logging data has been in use since the early 1960[4]. Today an extremely large variety of two and three dimensional cross-plots are available. There are many cross-plots models can be used for each formation to determine lithological type, such as mono, binary and triple-mineral. Assuming a reservoir rock of known lithology, which is clean and /or shale corrected, then each porosity value can be explained for cross-plots type [5]. By virtue of the different responses of matrix minerals to the individual porosity logs, immediate indications of the lithology of logged units will be given by an overlay of any combination of the three porosities. Hypothetical response of a mixed sequence of lithologies can be compare to the density, sonic, and neutron logs to illustrate this point.

3.2.1 Sonic and Neutron Logs Cross-Plot

A cross-plot of two porosity logs is convenient to display both porosity and lithology information. This cross-plot was constructed for clean, liquid saturated formation and boreholes filled with water or water-base mud.

The sonic-neutron cross-plot for Yamamma Formation is shown in Figure (11). This figure illustrates the separation between the sandstone, limestone and dolomite lines that indicate good resolution for these lithologies

3.2.2 Density and Neutron Cross-Plot

Density-sonic cross plot is the first cross-plot. As water-filled porosity increases, three different loci could be traced out for differing travel times and matrix densities for the three principal matrices. A considerable confusion in the ascribed lithology caused by a little uncertainty in the measured pair (Δ_t-ρ_b) means the contrast between the matrix endpoints is not a great deal. In addition, depending on the type of sonic transform used, there is a large difference as well [6, 7].

As in the previous cross-plot the density (RHO)-neutron (NPHI) cross plot is provided for clean fully liquid-saturated formations and holes filled with water or water based-mud. Figure (12) shows the density-neutron cross-plot for Yamamma Formation.

3.2.3 Ternary Porosity Model

Finally, the cross-plot as presented by Schlumberger is the lithology interpretation with neutron, density and sonic logs facilitated by use of M-N plots [5]. Before combining them, to deduce the matrix parameters the gross effect of porosity from the three measurements is removed. Due to matrix endpoints, the slope of the (Δ_t-ρ_b) time average curve presented by M varies slightly between the three major lithologies which are expressed as follows [6, 7].

$$M = \frac{\Delta t_f - \Delta t_{\log}}{\rho_b - \rho_f} \quad \text{.....(3)}$$

The neutron-density cross plot yields a similar slope, designated as N:

$$N = \frac{\Phi_{Nf} - \Phi_{N\log}}{\rho_b - \rho_f} \quad \text{.....(4)}$$

For fresh mud, Δt_f=189, ρ_f=1, and Φ_{Nf}=1

The M-N cross-plot is detected by lithology interpretation with neutron, sonic and density. It is a two-dimensional display of all three porosity logs responses in complex reservoirs rocks. M and N are lithology-dependent parameters but essentially independent of primary porosity therefore, a cross-plot of these two parameters makes porosity more apparent. The results are shown in Figure (13).

3.3 Determination of R_t, Rxo, R_w, and Rmf

True resistivity (R_t) may be obtained from DIL or DLL, so any invasion correction should be applied to obtain the true resistivity which will lead to good interpretation for water saturation [6].The resistivity of the flushing zone (Rxo) also had obtained from the Micro Spherical Focused Log (MSFL) tool and mud cake correction chart Rxo-3 [7]. The invasion correction charts, also referred to as (tornado) or (butterfly) charts, assume a step-contact

profile of invasion and that all resistivity measurements have already been corrected as necessary for borehole effect using IP software. The results are shown in Figure (14).

Formation Water Resistivity (R_w) and Mud Filtrate Resistivity (R_{mf}) the main parameters needed to calculate water saturation, movable hydrocarbon and permeability by conventional methods are R_w and R_{mf}, which can be obtained from connate water analysis and special core analysis, respectively. Core measurements are often expensive because they involve the cost of extracting the core sample and laboratory work [8]. In the present days, in the NS oil field formation evaluators are used the SP and resistivity logs in the borehole measurements for interpretation to log analysts or petrophysicist. The spontaneous potential log reading is described in the following equation [3]:

$$SSP = -K \log \frac{R_{mf}}{R_W} \quad (5)$$

R_{mfe}: equivalent mud filtrate resistivity, ohm-m.; R_{we}: equivalent formation water resistivity, ohm-m., and SP: spontaneous potential log reading, mv.

The apparent formation water resistivity (R_{Wa}) and apparent mud filtrate resistivity are obtained from the Archie's equation, which assumes clean water-bearing formation, so R_{wa} and R_{mfa} are defined by the following relationships [9]:

$$R_{Wa} = \frac{Rt}{F} \quad (6)$$

$$R_{mf} = \frac{R_{shallow}}{F} \quad (7)$$

The apparent formation water resistivity (R_{Wa}) and apparent mud filtrate resistivity are obtained from the Archie's equation, which assumes clean water-bearing formation [10]. Although this method gives sufficient results, but it is usually used as quick-look method to detect hydrocarbon zones, also it is used to determine R_w and R_{mf} in the absence of SP log or to do a double check for the result of R_w from SP [9]. The results of applying this method are shown in Figure (5). While the results of R_w and R_{mf} for this formation are shown in Table (2).

3.4 Determination of Archie's Parameters

Resistivity-porosity cross-plot method was used to calculate (*m* and a) from well logs using the following Pickett equation [11, 12].

$$\log R_t = -m \log \Phi + \log aR_w \quad (8)$$

Equation (8) is a straight line equation on log-log paper, where *m* is the slope and (a. R_W) is the intercept at Φ=1. As R_W is known from other sources, then (a) can easily find. The application of this method is shown in Figure (15) and the values of cementation factor, tortusity and saturation exponent from Pickett method and core analysis are listed in Table (2

3.5 Determination of Water Saturation

The determination of water saturation (S_w) is the most important step in log interpretation as all above work done to get more accurate water and hydrocarbon saturation. Archie in 1942 was introduced equation, which based on laboratory experiments on clean sands, water wettability and non- vugy carbonates, as follows [13]:

$$Sw^n = \frac{a.Rw}{Rt.\Phi^m} \quad (9)$$

3.6 Bulk Analysis of Formation Fluid

The following steps were used to calculate the bulk parameters [3].

1. Bulk of Free Water

$$BV_W = \Phi_e S_W \quad (10)$$

Φ_e is effective porosity.

2. Bulk of Flushed Zone Water

$$BVW_{SXO} = \Phi_e . S_{XO} \quad (11)$$

Figure (16) shows the results of computer process interpretation CPI plots, which represent the application of above equations.

Table 1. Core - log average porosity comparison results

Core no.	Depth Interval (m)	Reading no.	Φ_{cor}: Average core Porosity	Φ_{CPI}: Average CPI porosity
C1	3190.89-3191.28	2.0	0.0645	0.0588
C2	3209.04-3216.37	12	0.0749	0.0895
C3	3219.20-3226.80	5.0	0.0394	0.0491
C4	3234.5	1.0	0.0212	0.0191
C5	3251.50-3255.63	7.0	0.0971	0.0875
C6	3260.10-3264.35	7.0	0.0554	0.0776
C7	3277.14-3292.22	10	0.1630	0.128
C8	3293.21-3310 .29	27	0.134	0.141
C9	3310.33-3323.60	16	0.127	0.119
C10	3358.10-3363.84	11	0.153	0.139

Table 2. Resistivity results

Resistivity	R_w from SP log	R_w from R_{wa} method	R_w from water formation analysis	R_{mfa} from R_{mfa} method
Value	0.0172	0.0181	0.0178	0.0910

Table 3. Comparsion between core and Pickett method results

Parameter	m	a	n
Picket Value	1.89	0.96	2
Core Value	1.78	0.797	2

4. Discussion

Using IP software, corrections were achieved per 0.1524 m of depth to avoid erroneous results in water saturation interpretations. The correction charts (SLB, 2005) were supplied to the software as the environmental correction module. The environmental corrected results for porosity from density, sonic, and neutron logs are shown in Figure (1). The Computer Processed Interpretation (CPI) results of effective porosity (PHIE) are closed to the core data analysis as shown in Table (1) and Figures 2, 3, 4, 5, 6, 7 and 8 that means the porosity interpretation by porosity logging tools have good quality after making the environmental correction.

The relationship between core and CPI porosity is shown in Figure (9). From this figure the corrected equation for effective porosity was produced. This equation was used to correct the CPI value of the effective porosity as shown in Figure (10). The main reason that leads to differences between the porosity value from core and log is the varying between properties of formation water and the mud filtrate [14]**.** The Ferro Chrome Lignite - Chrome Lignite (FCL-CL) was used as drilling mud in the NS-3 well. The (FCL-CL) mud contains barite as a weighting agent and characterized by a high ratio of free phase (water), which lead to a high diameter of invasion zone (more than 50 in) ,that mean the investigation zone for logging tools was invaded by barite.

The sonic (DT)-Neutron porosity (NPHI) cross-plot for Yamamma formation provides a resolution between sandstone, limestone, anhydrite and dolomite lithologies. No secondary porosity effects were noticed since both logs measure total porosity. The clay effect is clearly noticed by shifting some points towards east and the bad-hole effects make some points to be scattered as shown in Figure (11).

The density (RHO)-neutron (NPHI) cross-plot provides satisfactory resolution of porosity and lithological

column. Here too, no secondary porosity effects were noticed for the same reason stated above. Also the non considerable shale effect is clearly noticed by shifting some points towards east as shown in Figure (12).

Figure (13) illustrates to the N-M plot points for several-single mineral Yamamma Formation. The M-N cross-plot shows that the Yamamma reservoir consists mainly of limestone although it is dolomitize in some places and there are traces of shale.

From Figure (14), can be seen that the resistivity tools for the selected well produced good results that listed in Table (2), due to that the data of R_{mf} and Rw are compatible with the following relationships [3]:

$$R_{mf}/ R_w > 2.5 \text{ and } R_{mf} >> R_w$$

This relationships are preferred for induction tools environment, otherwise the selection of induction tools was enormous wrong and the re-evaluation process must be made with other tool such as; the Dual Laterolog [3].

The values of Arche's parameters (*m*, a, n) which are estimated by Pickett method as shown in Figure (15) are almost close to the core samples values of NS-3 well. Cementation factor, tortusity and saturation exponent from Pickett method and core analysis are illustrated in Table (3).

From trake number three in Figure (16) the gamma ray tool in the CPI shows that there is no valuable shale effect along the depth interval from 3177m to 3403m of Yamammah formation. Approximately, most of the NS field wells that were interpreted by different CPI methods have used constant Archie parameters while, in fact, these parameters have different values especially in carbonate formations formations which affect fluid saturation. The constant values of Archie give low hydrocarbon saturation.

5. Conclusions

1. The difference in Archie parameters through the well depth reflects the heterogeneity of the studied area.
2. From deep invasion diameter, and low cementation exponent (below 2), it is concluded that the reservoir may be fractured naturally.
3. The resistivity tools were given good results according to the values of R_{mf} and R_w.
4. Gamma Ray tools detected there is no considerable shale volume in the Yamamma formation.
5. Cross-plots interpretations show that the Yamamma reservoir consists mainly of limestone, some dolomite.

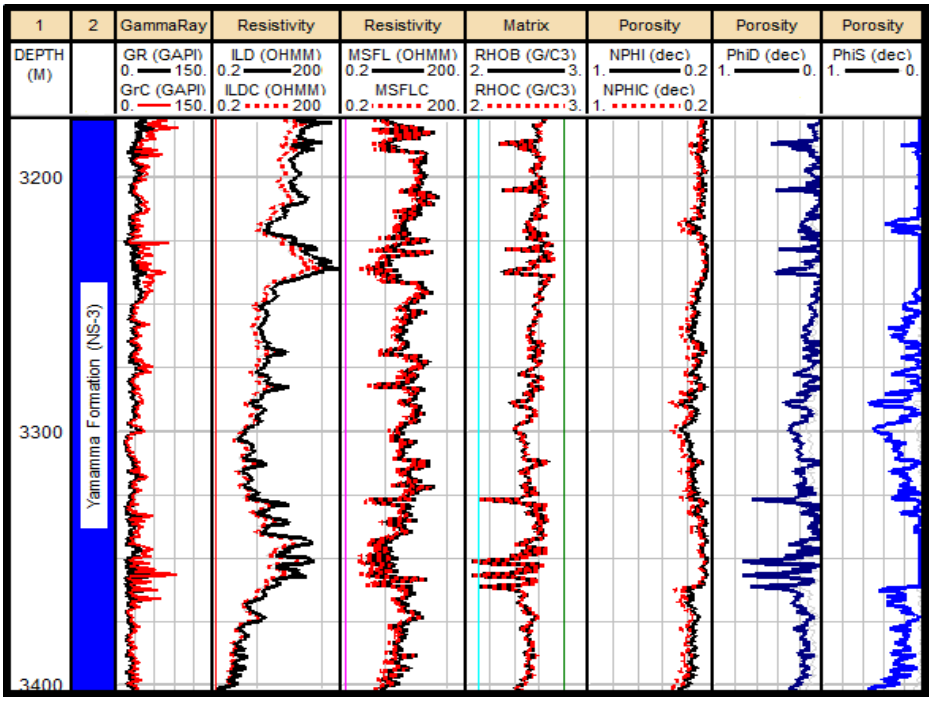

Figure 1. Environmental correction results of gamma ray, resistivity and neutron porosity logs (tracks 3 to 7) and porosity values from sonic and density logs (tracks 8 and 9)

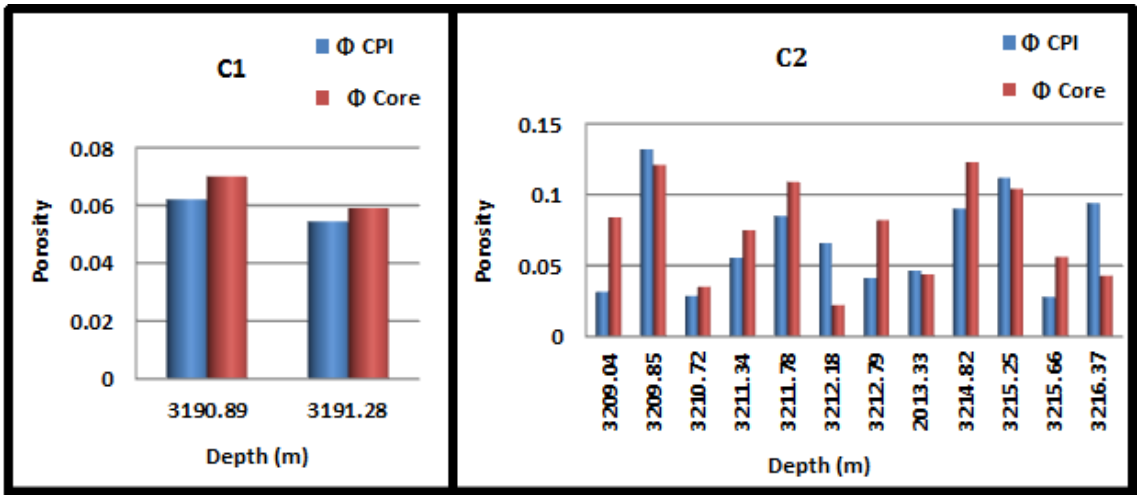

Figure 3. Comparison between core and CPI porosity results for C1and C2

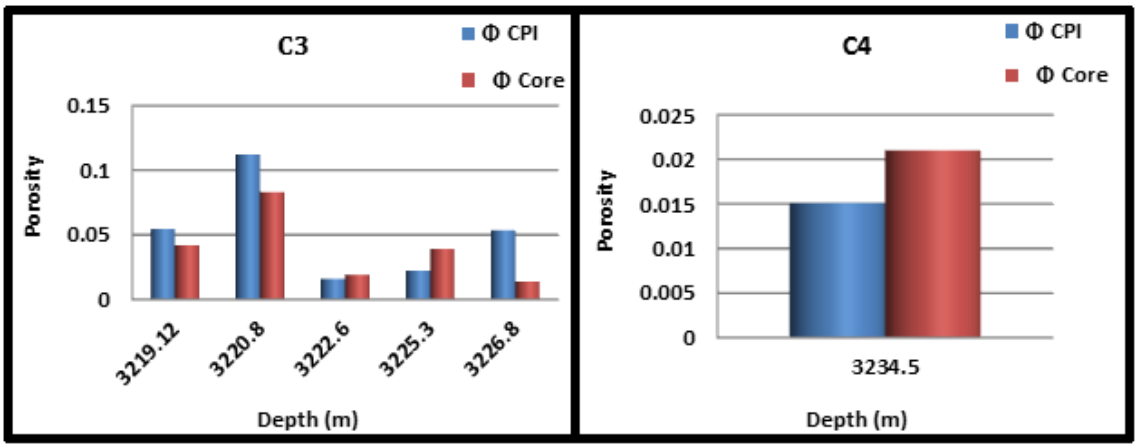

Figure 4a. Comparison between core and CPI porosity results for C3 and C4

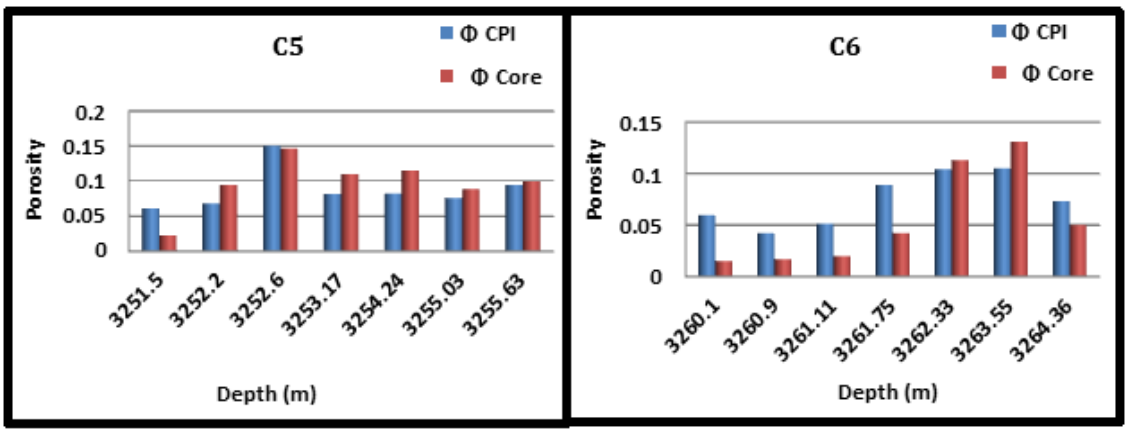

Figure 4b. Comparison between core and CPI porosity results for C5 and C6

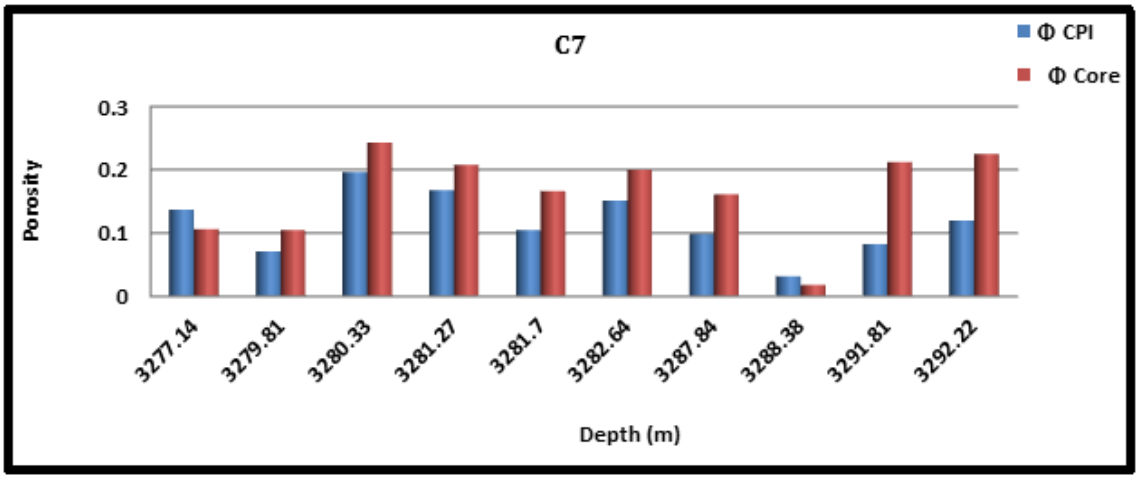

Figure 5. Comparison between core and CPI porosity results for C7

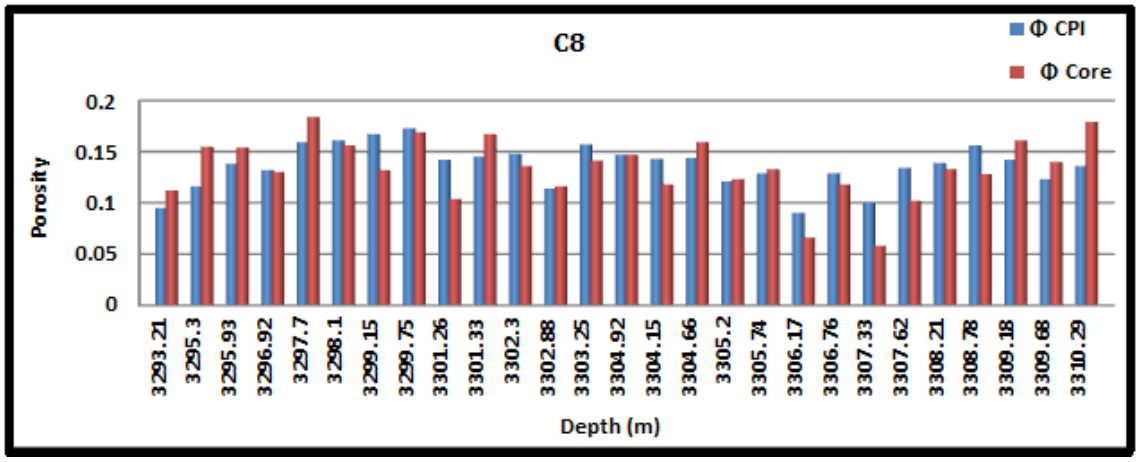

Figure 6. Comparison between core and CPI porosity results for C8

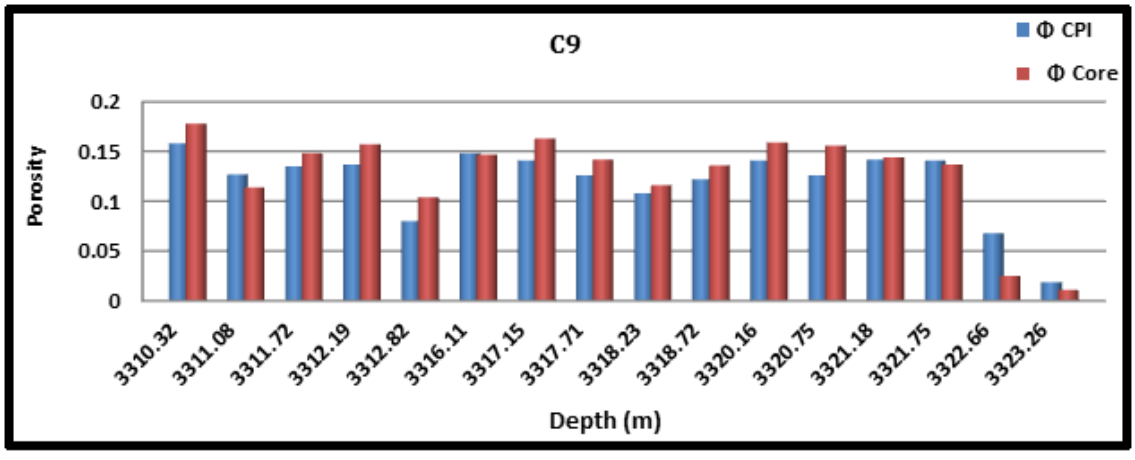

Figure 7. Comparison between core and CPI porosity results for C9

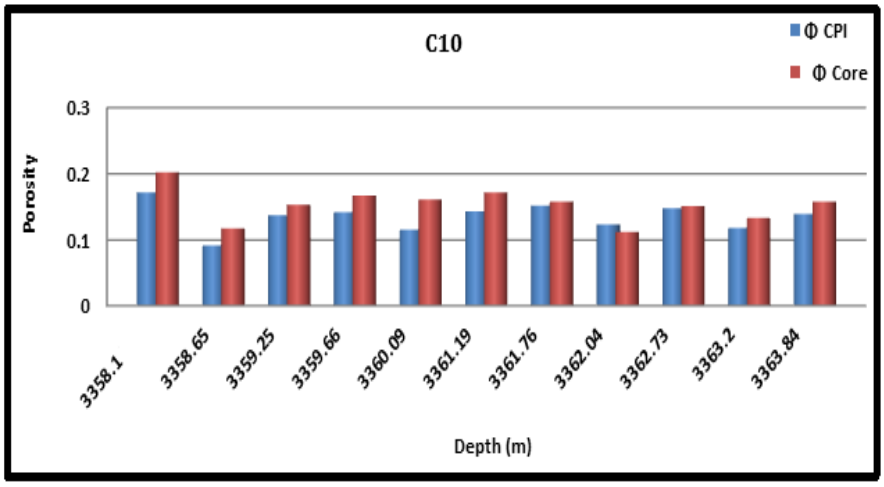

Figure 8. Comparison between core and CPI porosity results for C10

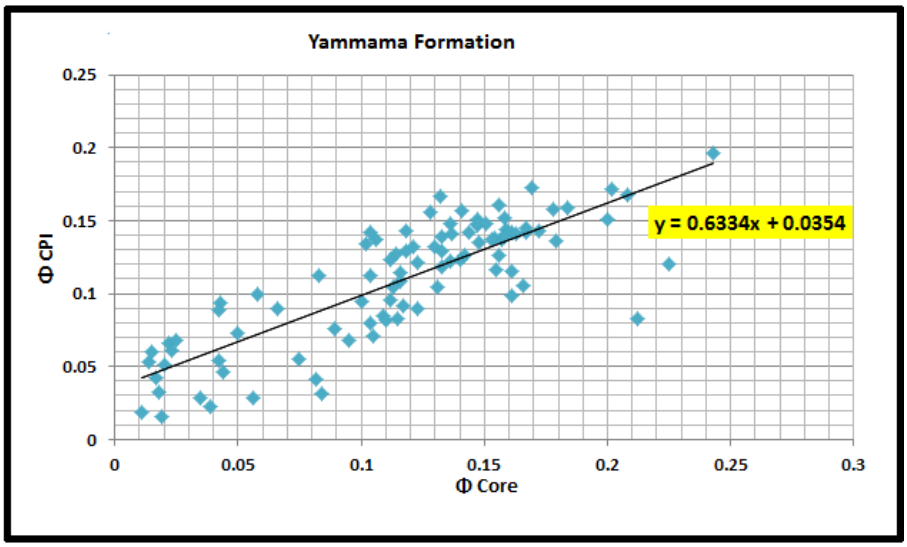

Figure 9. ΦCPI and ΦCore relationship to Yammama formation

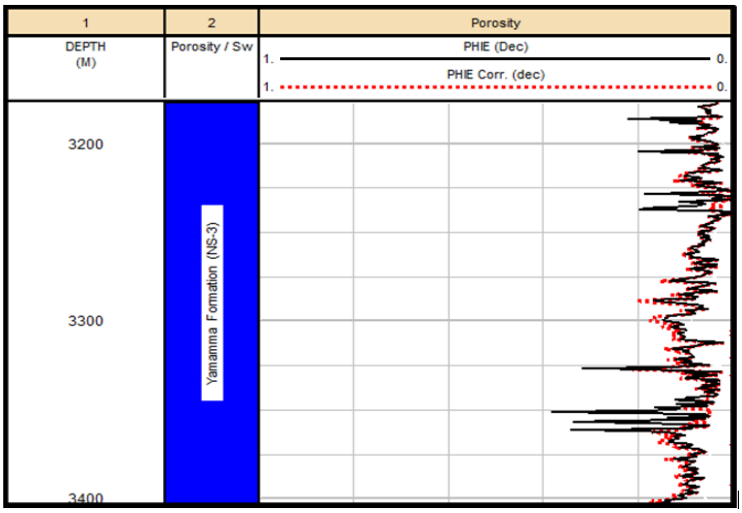

Figure 10. Effective porosity results as per core correction equation

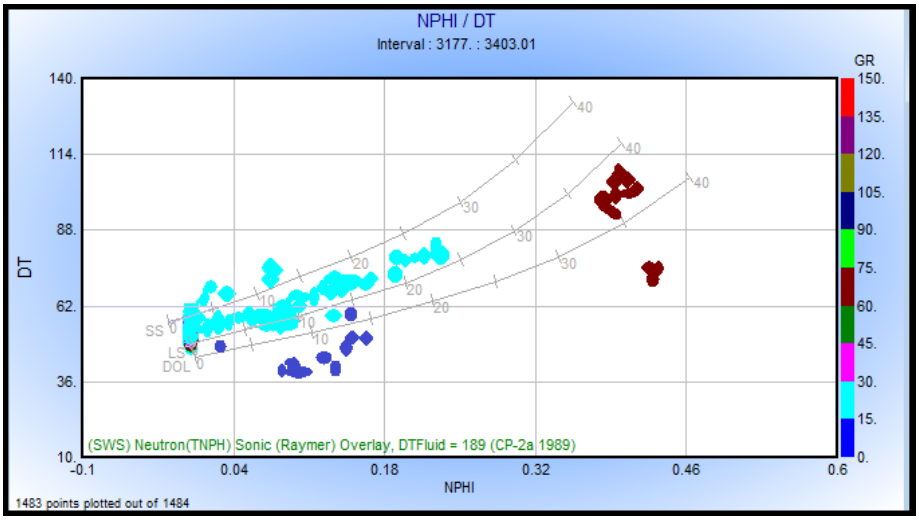

Figure 11. (DT) vs. (NPHI) cross plot

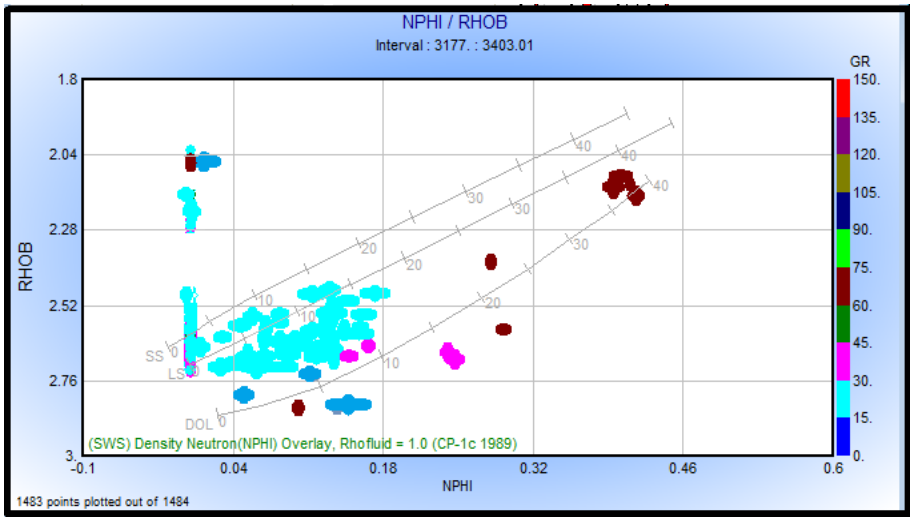

Figure 12. (RHO) vs. (NPHI) cross plot

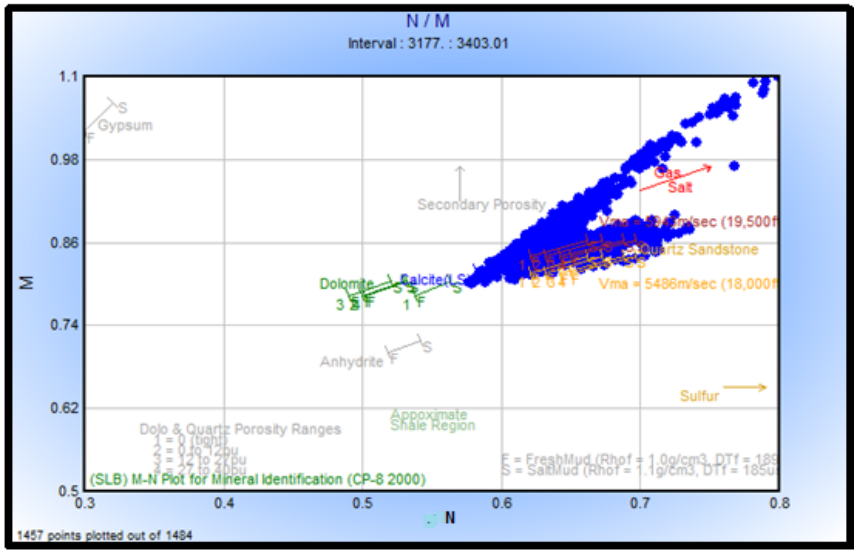

Figure 13. M vs. N cross plot

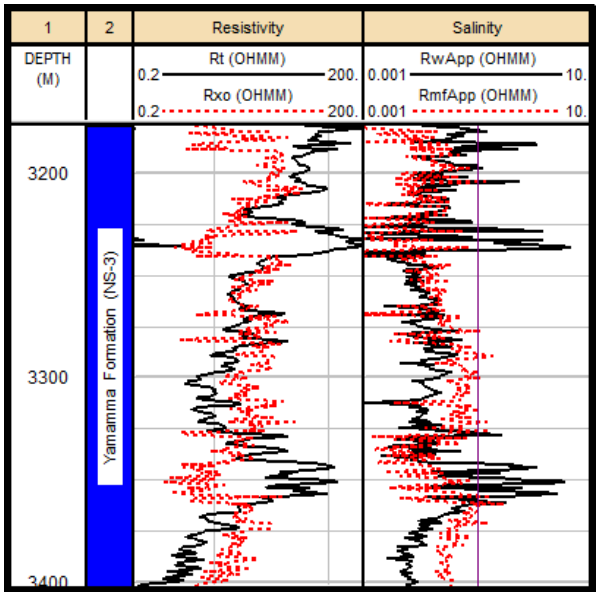

Figure 14. Rt, Rxo, Rwa, and Rmfa results

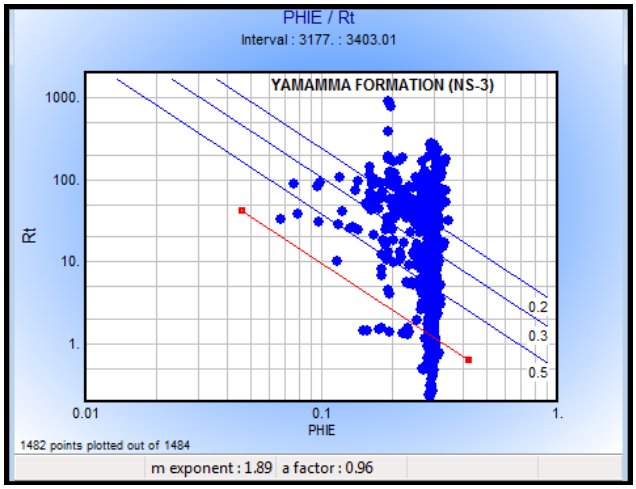

Figure 15. a, m values by Pickett method

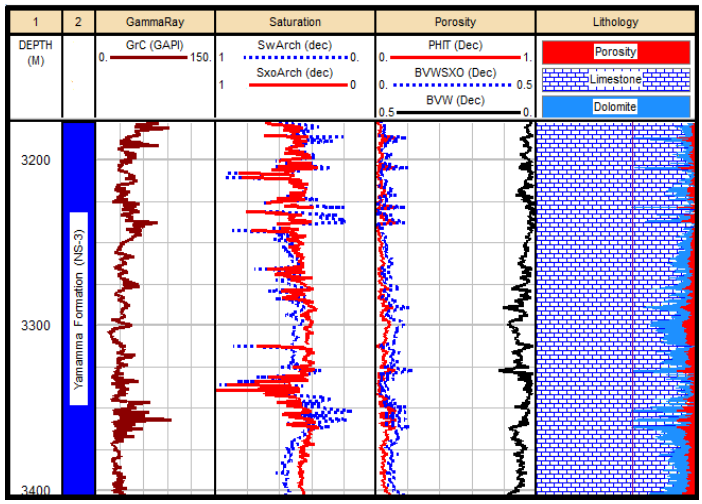

Figure 16. CPI plot for NS-3 well

Acknowledgments

The authors would like to thank the Ministry of Higher Education (MOHE) in Iraq for providing a research grant and Universiti Teknologi Malaysia (UTM) for supporting a research assistantship.

References

Amin, A. T, Watfa, M., & Awad. M. A. (1987). Accurate estimation of water saturation in complex carbonate reservoir, SPE-15714-MS: Society of Petroleum Engineers, presented at the 5th SPE Middle East Oil show in Bahrain, p.16.

Antwan, M. (1988). Well Log Analysis (pp. 187-235). Printed by Al-Mosul University. Mosul, Iraq.

Archie, G. E. (1942). The Electrical Resistivity Logs as an Aid in determining some Reservoir Characteristics. SPE-942054-G.

Bessiouni, Z. (1994). Theory, Measurement and Interpretation of Well Logs. *SPE Text Book series, 4*, 1-13.

Darwin, V. E., & Julian, M. S. (2007). *Well Logging for Earth Scientists* (2nd Ed.). Springer, the Netherlands, pp 629-634.

Etnyre, L. M. (1989). Finding Oil and Gas from Well Logs (pp. 72-76). Van Nostrand Renhold, New York.

Gilchrist, W. A., & Baker, H. (2008). Compensated Neutron Log Response Issues – A Tutoria (pp. 1-11). 49th Annual Logging Symposium, SPAWLA-2008-S, Edinburgh, Scotland.

Jesús Salazar, M., Wang, G. L., Carlos, T., & Lee, H. J. (2007). Combined Simulation and Inversion of SP and Resistivity Logs for The Estimation of Connate Water Resistivity and Archie's Cementation Exponent. 48th Annual Logging Symposium, SPAWLA-2007-H, Austin, Texas, 1-12.

Kadhim, F. S., Samsuri, A., & Kamal, A. (2013). A review in correlation between cementation factor and carbonate rock properties. *Life Sci. J, 10*(4), 2451-2458.

Mazzullo, S. J. (1986). Stratigraghic approach of hydrocarbon exploration and exploitation. *Geol. J., 21,* 265-28.

Morries, R. L., & Biggs, W. P. (1967). Using log-derived values of water saturation and porosity (pp. 1-26). 8th Annual Logging Symposium, SPWLA-1967 -X. Denver, Colorado.

Pickett, G. R. (1966). A Review of Current Technique for Determination of water saturation from Logs. SPE1446.

Richard, G. C. (1963). Principles of log Interpretation by Use of Multiple Curves (pp. 1-22). 49th Annual Logging Symposium, SPAWLA-1963-E, Oklahoma.

Toby, D. (2005). Well Logging and Formation Evaluation (pp. 37-40). Elsevier. Boston.